

Structural alterations of the choroid evaluated using enhanced depth imaging optical coherence tomography in patients with coronavirus disease

Alterações estruturais da coroide avaliadas por imagens de tomografia de coerência óptica com profundidade realçada em pacientes com COVID-19

Özkan Kocamış¹, Emine Temel² , Lokman Hızmalı³, Nazife Aşıkgarip², Kemal Örnek¹ , Fikriye Milletli Sezgin⁴

1. Department of Ophthalmology, Kırşehir Ahi Evran University School of Medicine, Kırşehir, Turkey.

2. Department of Ophthalmology, Kırşehir Ahi Evran Training and Research Hospital, Kırşehir, Turkey.

3. Department of Infectious Disease and Clinical Microbiology, Kırşehir Ahi Evran University School of Medicine, Kırşehir, Turkey.

4. Department of Medical Microbiology, Kırşehir Ahi Evran University School of Medicine, Kırşehir, Turkey.

ABSTRACT | Purpose: To assess choroidal changes using enhanced depth imaging optical coherence tomography in coronavirus disease (COVID-19). **Methods:** Thirty-two patients with moderate COVID-19 and 34 healthy subjects were included in the study. Choroidal thickness was measured at 3 points as follows: at the subfovea, 1500 mm nasal to the fovea, and 1500 mm temporal to the fovea. The total choroidal area, luminal area, stromal area, and choroidal vascular index were measured with Image-J. All the measurements were performed during the disease and at 4 months after remission. **Results:** In the patient group, the subfoveal, nasal, and temporal choroidal thicknesses were decreased as compared with those in the controls, but without statistically significant differences ($p=0.534$, $p=0.437$, and $p=0.077$, respectively). The mean total choroidal, stromal, and luminal areas and choroidal vascular index were statistically significantly decreased in the patient group ($p<0.001$, $p=0.001$, $p=0.001$, and $p=0.003$; respectively). At 4 months after remission, the choroidal structural parameters and choroidal vascular index revealed statistically significant increases as compared with the baseline measurements in the patients with COVID-19 (all $p<0.001$ and $p=0.047$, respectively). **Conclusion:** The choroidal vascular and stromal parameters showed significant transient decreases during the disease course of COVID-19.

Keywords: Choroid; COVID-19; Coronavirus infections; tomography, optical coherence

RESUMO | Objetivo: Avaliar alterações da coroide através de imagens de tomografia de coerência óptica (OCT) com profundidade realçada na doença por coronavírus de 2019 (COVID-19). **Métodos:** Foram incluídos no estudo 32 pacientes com COVID-19 moderada e 34 indivíduos saudáveis. A espessura da coroide foi medida em 3 pontos: subfoveal, a 1500 mm da fóvea na direção nasal e a 1500 mm da fóvea na direção temporal. A área total da coroide, a área luminal, a área estromal e o índice vascular da coroide foram medidos com o programa ImageJ. Todas as medições foram feitas durante a doença ativa e 4 meses após a remissão. **Resultados:** No grupo de pacientes, as espessuras subfoveal, nasal e temporal da coroide mostraram-se reduzidas em comparação com os controles. A diferença não foi estatisticamente significativa (respectivamente, $p=0,534$, $p=0,437$ e $p=0,077$). As médias das áreas total da coroide, estromal e luminal, bem como o índice vascular da coroide, mostraram-se diminuídos com significância estatística no grupo de pacientes (respectivamente, $p<0,001$, $p=0,001$, $p=0,001$ e $p=0,003$). Aos 4 meses após a remissão, os parâmetros estruturais e o índice vascular da coroide revelaram um aumento estatisticamente significativo em pacientes com COVID-19, em comparação com as medidas iniciais (todos os valores de $p<0,001$ para os parâmetros estruturais e $p=0,047$ para o índice vascular da coroide). **Conclusão:** Os parâmetros vasculares da coroide e do estroma mostraram uma diminuição transitória, mas significativa em pacientes com COVID-19 durante a doença.

Descritores: Coróide; COVID-19; Infecções por coronavírus; Tomografia de coerência óptica

INTRODUCTION

Coronavirus disease (COVID-19) is extremely contagious, causing severe acute respiratory distress syndrome, and can lead to death especially in patients with con-

Submitted for publication: August 25, 2020

Accepted for publication: February 19, 2021

Funding: This study received no specific financial support.

Disclosure of potential conflicts of interest: None of the authors have any potential conflicts of interest to disclose.

Corresponding author: Emine Temel.

E-mail: emine912@hotmail.com

Approved by the following research ethics committee: Kırşehir Ahi Evran University School of Medicine (# 2020-10/79).

 This content is licensed under a Creative Commons Attributions 4.0 International License.

comitant systemic disease⁽¹⁾. The disease has rapidly become widespread, resulting in an epidemic throughout China, followed by a pandemic, with an increasing number of cases in various countries worldwide⁽²⁾.

The exact pathophysiological mechanism of the COVID-19 infection remains largely unknown. However, it has been proposed that during the disease course, immune dysregulation and the high levels of proinflammatory cytokines could be the main cause of tissue injury⁽³⁾. In addition, some studies showed that vascular damage, thrombosis, and dysregulation of immune-mediated inflammation play important roles in the pathogenesis of severe COVID-19 infection⁽⁴⁾.

COVID-19 has been shown to affect different parts of the body. However, current studies on the ocular effects of COVID-19 are limited. As far as we know, ophthalmic changes are limited to external diseases such as conjunctivitis⁽⁵⁻⁷⁾. Furthermore, ocular manifestations such as retinitis, uveitis, and optic neuritis have been reported to occur owing to coronavirus infections in various animal models⁽⁸⁾. Casagrande et al. showed that viral ribonucleic acid is detectable in the retina of patients with COVID-19⁽⁹⁾.

Enhanced depth imaging optical coherence tomography (EDI-OCT) is a noninvasive imaging tool that enables visualization of retinal and choroidal structural alterations in numerous ocular and systemic conditions^(10,11). Considering that COVID-19 has been shown to cause vascular dysfunction and inflammation, we hypothesized that the disease may also affect the choroid and its stromal and vascular structures. Therefore, the aim of our study was to assess choroidal structural changes using EDI-OCT and Image-J in patients with COVID-19.

METHODS

Patient selection

This prospective cross-sectional study included patients who were hospitalized for confirmed COVID-19 at the Kırşehir Ahi Evran University Training and Research Hospital. A total of 32 COVID-19 patients (32 eyes, group 1) and 34 healthy subjects (34 eyes, group 2) were included in the study. All the patients were positive for COVID-19 in real-time reverse transcriptase-polymerase chain reaction tests using nasopharyngeal swabs.

The study was performed in adherence to the tenets of the Declaration of Helsinki and was approved by the institutional review board of the Kırşehir Ahi Evran University School of Medicine (Decision number: 2020-

10/79). Each patient was informed about the aims and methods of the study, and informed consent was obtained from all the patients.

All the patients had moderate COVID-19. The criteria for hospitalization were dyspnea (shortness of breath at rest), oxygen saturation <90%, and symptoms of hypoxia (mental confusion, coughing, severe headache, and tachycardia) with abnormal laboratory findings. None of the patients in the study were admitted to the intensive care unit. The treatment protocol included oral hydroxychloroquine and favipiravir for 5 days and subcutaneous enoxaparin sodium for 1 month. None of the patients had any other blood flow examinations such as color Doppler imaging during hospitalization.

The right eye of each patient was included in the study. The exclusion criteria were as follows: retinal diseases such as retinal vascular occlusive disease, hypertensive retinopathy, diabetic retinopathy, central serous chorioretinopathy, age-related macular degeneration, degenerative myopia, intraocular pressure >22 mmHg, any systemic abnormalities (e.g., vascular disease, hypertension, or diabetes mellitus), history of previous intraocular surgery or laser photocoagulation, smoking, several types of systemic medication, and caffeine intake. Patients with poor-quality EDI-OCT images due to corneal or lens opacities were also excluded from the study.

Imaging and image analysis

Slit-lamp biomicroscopy and EDI-OCT (Spectralis, Heidelberg Engineering Inc., Heidelberg, Germany) measurements were performed by the ophthalmologists while wearing full protective equipment in group 1. The same measurements were also performed for the eyes included in the control group.

Choroidal thickness was measured from the outer portion of the hyperreflective line, corresponding to the retinal pigment epithelium, to the inner surface of the sclera. The choroidal thickness measurements were made at the following 3 points: at the subfovea, 1500 µm nasal to the fovea, and 1500 µm temporal to the fovea (Figure 1). EDI-OCT images were recorded at the same time of the day (9:00 am to 12:00 pm) to avoid the influence of diurnal variations. All the measurements were performed by 2 independent masked observers at baseline and 4 months after remission.

Binarization of the choroidal area was performed with the Image-J Version 1.50a software (National Institutes of Health, Bethesda, MD, USA; Figures 2 and 3).

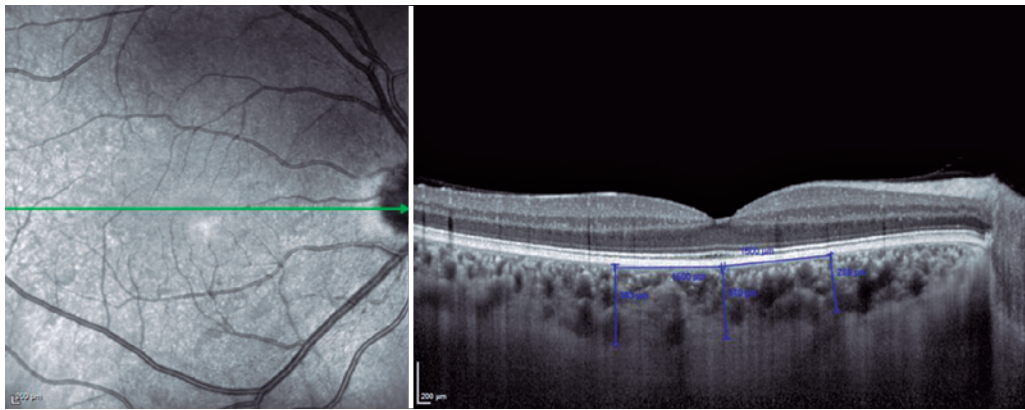


Figure 1. Choroidal thickness measurements at 3 points as follows: at the subfovea, 1500 μm nasal to the fovea, and 1500 μm temporal to the fovea.

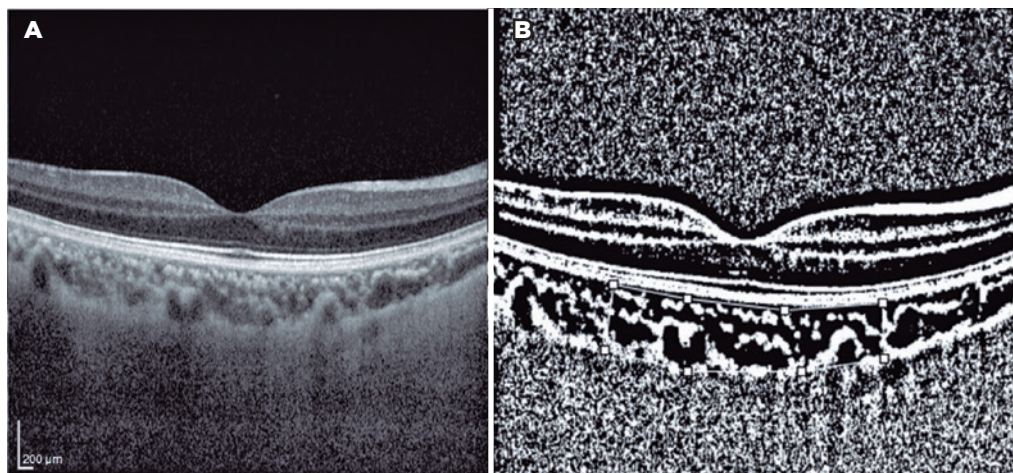


Figure 2. (A) Enhanced depth imaging optical coherence tomography image of the eye of a healthy subject. (B) Converted binary image using Image-J, with the area of interest in the choroid demarcated with a white line. The choroidal area was measured at approximately 3000 μm wide, with margins of 1500 μm nasal and 1500 μm temporal to the foveal center. The light pixels were evaluated as the stromal area; and the dark pixels, as the luminal area.

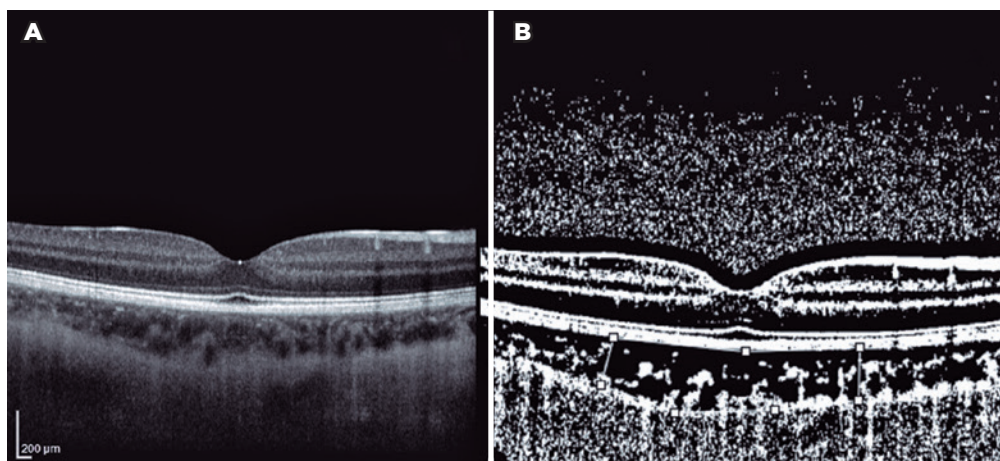


Figure 3. (A) Enhanced depth imaging optical coherence tomography image of the eye of a patient with COVID-19 infection. (B) Converted binary image using Image-J, with the area of interest in the choroid demarcated with a white line. The choroidal area was measured at approximately 3000 μm wide, with margins of 1500 μm nasal and 1500 μm temporal to the foveal center. The light pixels were evaluated as the stromal area; and the dark pixels, as the luminal area.

The EDI-OCT image was opened with Image-J, and 3000- μm wide areas with margins of 1500 μm temporal to the fovea was chosen. The choroidal area was defined as the region from the retinal pigment epithelium to the choriocleral border, and the borders were set manually with the Image-J ROI Manager. Three choroidal vessels with lumens $>100 \mu\text{m}$ were selected using the oval selection tool and the mean reflectivity of the luminal areas were determined. The Niblack method was used for the binarization of the choroidal image. Then, the image was converted to 8 bits and adjusted using the Niblack auto local threshold. The luminal area was determined with the threshold tool. After adding the distance between the pixels, the choroidal, luminal, and stromal areas were automatically calculated for the 2 groups. The light pixels were accepted as the stromal area; and the dark pixels, as the luminal area⁽¹²⁾. The choroidal vascularity index (CVI) was calculated as the ratio between the luminal and total choroidal areas.

Statistical analyses

All the comparisons between the 2 groups were statistically analyzed using SPSS 11.5 (SPSS Inc., Chicago, IL, USA). The normality of all the data was tested with the Kolmogorov-Smirnov test. The significance of the differences between the groups was investigated using one-way analysis of variance and the Kruskal-Wallis test. Pairwise comparisons with the Tukey HSD and Bonferro-ni tests were used to evaluate which group had significant differences. Intraclass correlation coefficients were used for the assessment of the reliability of all the measurements. Statistical significance was set at $p < 0.05$.

RESULTS

Of the patients with COVID-19, 14 (43.7%) were female, and the mean age was 35.9 ± 21.6 years (range: 8-87 years). Twenty (58.8%) of the patients in the control group were female, and the mean age was 37.2 ± 14.9 years (range: 10-63 years). No statistically significant differences were found between the 2 groups in terms of age and sex ($p=0.667$ and $p=0.452$, respectively). Table 1 shows the demographic and clinical data of the patients with COVID-19 and healthy subjects.

Of the patients with COVID-19, 7 (21.9%) had abnormal findings on computed chest tomography. Two patients (28.6%) with abnormal chest tomography findings had symptoms such as cough and shortness of breath. In addition, among the patients with COVID-19, 5 (15.6%)

Table 1. Demographic and clinical data of the patients with COVID-19 (group 1) and healthy subjects (group 2)

| | Group 1 | Group 2 |
|------------------------------------|---------------------------|----------------------------|
| Patients, n (%) | 32 (48.5) | 34 (51.5) |
| Eyes, n (%) | 32 (48.5) | 34 (51.5) |
| Female, n (%) | 14 (43.7) | 20 (58.8) |
| Male, n (%) | 18 (56.2) | 14 (41.2) |
| Age (years), mean \pm SD (range) | 35.9 ± 21.6 (8-87) | 37.2 ± 14.9 (10-63) |

had abnormal laboratory findings such as elevated C-reactive protein level and reduced number of lymphocytes. No drug-related adverse effects were observed in the patients with COVID-19 during the treatment and follow-ups.

None of the patients, both symptomatic/asymptomatic and those with abnormal chest tomography findings, had coexisting ocular symptoms or findings. No abnormalities were found on the ocular surface and in the anterior chamber or posterior segment on slit-lamp examination.

The mean subfoveal choroidal thickness was $311.21 \pm 74.10 \mu\text{m}$ in the patient group and $322.91 \pm 77.56 \mu\text{m}$ in the controls. The mean choroidal thickness at 1500 μm nasal to the fovea was $260.31 \pm 80.62 \mu\text{m}$ in the patient group and $274.29 \pm 64.21 \mu\text{m}$ in the controls. The mean choroidal thickness at 1500 μm temporal to the fovea was $261.71 \pm 74.27 \mu\text{m}$ in the patient group and $297.73 \pm 87.57 \mu\text{m}$ in the controls. In the patients, the subfoveal, 1500- μm nasal, and 1500- μm temporal choroidal thicknesses were decreased as compared with those in the healthy subjects. No statistically significant differences were found between the 2 groups ($p=0.534$, $p=0.437$, and $p=0.077$, respectively). The distribution of choroidal thickness changes among groups is shown in figure 4.

According to the Image-J data, the mean total choroidal area was $0.540 \pm 0.17 \text{ mm}^2$ in the patient group and $0.957 \pm 0.21 \text{ mm}^2$ in the controls, with a statistically significant difference ($p < 0.001$). The mean stromal area was $0.164 \pm 0.05 \text{ mm}^2$ in the patient group and $0.229 \pm 0.08 \text{ mm}^2$ in the controls. The mean stromal area was decreased statistically significantly in the patients with COVID-19 ($p=0.001$). The mean luminal area was $0.376 \pm 0.15 \text{ mm}^2$ in the patient group and $0.727 \pm 0.16 \text{ mm}^2$ in the controls. When compared, the values showed a statistically significant difference ($p=0.001$).

The mean CVI was 67.91 ± 6.2 in the patient group and 76.11 ± 8.1 in the control group. The mean CVI was statistically significantly decreased in the patient group as compared with the healthy subjects ($p=0.003$). The distribution of CVI changes between the groups is shown in figure 5. Table 2 lists the choroidal structural characteristics of the patients with COVID-19 and healthy subjects.

At 4 months after remission, the CVI and choroidal structural parameters showed statistically significant increases as compared with the baseline values ($p=0.047$ and all $p<0.001$, respectively; Table 3), but no statistically significant differences were found between the patient and control groups (all $p>0.05$) (Table 4). The intraclass correlation coefficient and confidence intervals of all the measurements are listed in table 5.

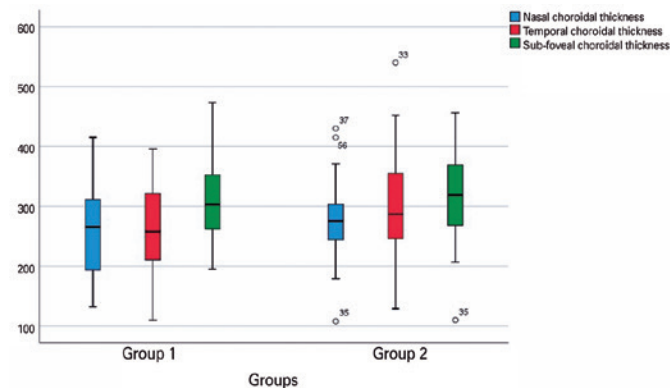


Figure 4. The distribution of choroidal thickness changes detected on the enhanced depth imaging optical coherence tomography images of the patients with COVID-19 (group 1) and healthy subjects (group 2).

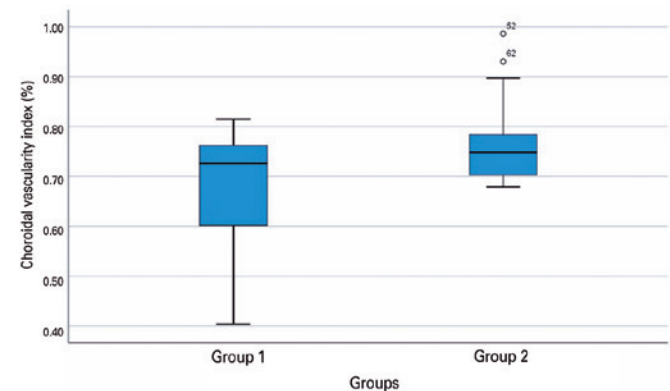


Figure 5. Distribution of CVI changes detected using binarization of the enhanced depth imaging optical coherence tomography images of patients with COVID-19 (group 1) and healthy subjects (group 2).

DISCUSSION

Coronavirus has been shown to manifest in different parts of the human body, including the gastrointestinal system and eye, besides the respiratory system^(13,14). Most clinical studies about coronavirus have focused on the respiratory system because of its life-threatening nature. Evaluation of other organ systems should be taken into consideration, as it may help to provide valuable information for uncovering the obscure mechanisms of tissue injury.

Ocular involvement in patients with COVID-19 is limited to the conjunctiva and tear film layer, as reported in previous studies^(5,6,15). Viral ribonucleic acid can be detected in the retina of people with the infection⁽⁹⁾. In a study by Seah et al., coronaviruses were shown to produce various ocular manifestations ranging from anterior segment pathologies such as conjunctivitis and anterior uveitis to vision-threatening conditions such as retinitis and optic neuritis⁽⁸⁾.

The factors that trigger severe disease in individuals with COVID-19 infection are not completely understood. Hyperinflammation and coagulopathy have been shown to contribute to disease severity and death in patients with COVID-19⁽¹⁶⁾. In addition, clinical studies suggest that severe COVID-19 infection reflects a confluence of vascular dysfunction and disruption in thrombotic mechanisms⁽⁴⁾.

The choroid is the vascular part of the eye and plays an important role in the pathogenesis of several ocular diseases. The choroidal circulation is a dense network of capillaries located behind the retinal pigment epithelial cell layer. The choriocapillaris, which forms the innermost layer of the choroid, is the fundamental blood supply to the outer retina. Owing to the high metabolic demand of the photoreceptor layer, the choroid receives most of the blood (65-85%) supplied to the retinal structures⁽¹⁷⁾.

Impaired choroidal blood flow is associated with several ocular diseases such as glaucoma, retinitis pigmentosa, degenerative myopia, and age-related macular degeneration. Histological analysis has revealed that changes in the choroidal interstitial stroma may occur in eyes with age-related macular degeneration due to edema, fibrosis, and inflammation with cellular infiltration⁽¹⁸⁾.

In the present study, we compared the luminal and stromal areas of the choroid in patients with COVID-19 and healthy subjects by using the binarization technique

Table 2. Choroidal structural characteristics of the patients with COVID-19 (group 1) and healthy subjects (group 2)

| Variable (Mean ± SD) | Group 1 | Group 2 | p value |
|---|----------------|----------------|---------|
| Subfoveal choroidal thickness (µm) | 311.21 ± 74.10 | 322.91 ± 77.56 | 0.534 |
| Choroidal thickness at 1500 µm nasal to the fovea (µm) | 260.31 ± 80.62 | 274.29 ± 64.21 | 0.437 |
| Choroidal thickness at 1500 µm temporal to the fovea (µm) | 261.71 ± 74.27 | 297.73 ± 87.57 | 0.077 |
| Total choroidal area (mm ²) | 0.540 ± 0.17 | 0.957 ± 0.21 | <0.001* |
| Stromal area (mm ²) | 0.164 ± 0.05 | 0.229 ± 0.08 | 0.001* |
| Luminal area (mm ²) | 0.376 ± 0.15 | 0.727 ± 0.16 | 0.001* |
| CVI (%) | 67.91 ± 6.2 | 76.11 ± 8.1 | 0.003* |

SD= Standard deviation; CVI= Choroidal vascularity index.

* = Statistically significant p values.

Table 3. Comparison of the choroidal structural characteristics at baseline and after the remission period in the patients with COVID-19

| | Mean±SD | | p value |
|---|----------------|----------------|---------|
| | Baseline | Remission | |
| Subfoveal choroidal thickness (µm) | 311.21 ± 74.10 | 316.18 ± 64.12 | 0.662 |
| Choroidal thickness at 1500 µm nasal to the fovea (µm) | 260.31 ± 80.62 | 268.24 ± 78.21 | 0.554 |
| Choroidal thickness at 1500 µm temporal to the fovea (µm) | 261.71 ± 74.27 | 279.32 ± 69.43 | 0.332 |
| Total choroidal area (mm ²) | 0.540 ± 0.17 | 0.881 ± 0.086 | <0.001* |
| Stromal area (mm ²) | 0.164 ± 0.05 | 0.223 ± 0.07 | <0.001* |
| Luminal area (mm ²) | 0.376 ± 0.15 | 0.658 ± 0.113 | <0.001* |
| CVI (%) | 67.91 ± 6.2 | 74.84 ± 8.7 | 0.047* |

SD= Standard deviation; CVI= Choroidal vascularity index.

* = Statistically significant p value.

Table 4. Comparison of the choroidal structural characteristics after the remission period between the patients with COVID-19 and the controls

| | Mean ± SD | | p value |
|---|----------------------|----------------|---------|
| | Patients (Remission) | Controls | |
| Subfoveal choroidal thickness (µm) | 316.18 ± 64.12 | 322.91 ± 77.56 | 0.523 |
| Choroidal thickness at 1500 µm nasal to the fovea (µm) | 268.24 ± 78.21 | 274.29 ± 64.21 | 0.498 |
| Choroidal thickness at 1500 µm temporal to the fovea (µm) | 279.32 ± 69.43 | 297.73 ± 87.57 | 0.232 |
| Total choroidal area (mm ²) | 0.881 ± 0.086 | 0.957 ± 0.21 | 0.065 |
| Stromal area (mm ²) | 0.223 ± 0.07 | 0.229 ± 0.08 | 0.756 |
| Luminal area (mm ²) | 0.658 ± 0.113 | 0.727 ± 0.16 | 0.061 |
| CVI (%) | 74.84 ± 8.7 | 76.11 ± 8.1 | 0.385 |

SD= Standard deviation; CVI= Choroidal vascularity index.

* = Statistically significant p value.

Table 5. Intraclass correlation coefficient and confidence intervals of all the measurements

| | Cronbach's alpha coefficient | 95% CI | |
|---|------------------------------|--------|-------|
| | | Lower | Upper |
| Subfoveal choroidal thickness (µm) | 0.996 | 0.992 | 0.998 |
| Choroidal thickness at 1500 µm nasal to the fovea (µm) | 0.995 | 0.992 | 0.997 |
| Choroidal thickness at 1500 µm temporal to the fovea (µm) | 0.996 | 0.993 | 0.998 |
| Total choroidal area (mm ²) | 0.997 | 0.993 | 0.998 |
| Stromal area (mm ²) | 0.972 | 0.942 | 0.986 |
| Luminal area (mm ²) | 0.998 | 0.998 | 0.999 |
| CVI (%) | 0.997 | 0.994 | 0.999 |

CI= Confidence interval; CVI= Choroidal vascularity index.

with Image-J. Our findings showed that the mean total choroidal, luminal, and stromal areas were statistically significantly decreased in the patients with COVID-19 as compared with the healthy subjects.

Choroidal thickness is a parameter that varies substantially in both healthy and pathological conditions. It decreases from the macula to the periphery and is at its maximum subfoveally. Choroidal thickness does not provide a true representation of the entire choroidal vasculature as an objective marker. Measuring CVI provides information about the vascular and stromal components of the choroid. Xin et al. reported that CVI was independent from systemic and ocular factors such as age, axial length, intraocular pressure, or systolic blood pressure⁽¹⁹⁾. However, choroidal thickness may vary depending on these factors. In a study by Xin et al., the mean CVI reported for healthy subjects was 70.12%⁽¹⁹⁾. In our study, this ratio was 76.11% in the controls. Agarwal et al. found in their study that the subfoveal CVI was 65.61% by including 345 eyes of healthy subjects with a mean age of 61 years⁽²⁰⁾. In our study, we found a CVI of 76.11%, but the mean age of our control group was 37 years. The normative CVI value in healthy people was studied, and age-related changes were evaluated for CVI^(21,22). Jaeryung et al. showed no significant correlations between CVI and age⁽²¹⁾. By contrast, Ruiz-Medrano et al. reported that CVI was significantly higher in subjects aged 18 years than in a group of older people⁽²²⁾.

Some studies have reported regarding CVI and its potential applications in the evaluation, diagnosis, and treatment of diseases of the retina and choroid, such as central serous chorioretinopathy, polypoidal choroidal vasculopathy, panuveitis, and diabetic retinopathy⁽²³⁻²⁷⁾. Agrawal et al. assessed CVI in people with posterior uveitis and panuveitis and showed an increased CVI in the affected eye, which had significantly decreased at 3-month follow-up⁽²⁵⁾. Significant choroidal changes such as decreased CVI were also reported in eyes with serpiginous choroiditis associated with tuberculosis⁽²⁷⁾. Shulin et al. demonstrated a lower CVI during the active period of the Vogt-Koyanagi-Harada disease and hypothesized that decreased CVI during the active period was due to choroidal stromal edema and infiltration by inflammatory cells⁽²⁸⁾.

In our study, we observed that the mean CVI was decreased in the patients with COVID-19 infection as compared with healthy subjects. According to our hypothesis, vascular damage, hypercoagulability, and hyperinflammation factors, which have been shown to

be involved in the pathogenesis of COVID-19 infection, might have led to ischemia of the choriocapillaris and decreased CVI. In addition, the reduction in the luminal and stromal areas and CVI measured with Image-J might be explained by a secondary consequence of decreased oxygen demand. At 4 months after remission, the values all the choroidal parameters were increased close to the levels of the control group.

We also compared choroidal thickness changes between the patient and control groups. The subfoveal, 1500- μ m nasal, and 1500- μ m temporal choroidal thicknesses were decreased in the patients with COVID-19. Although the choroidal thickness was decreased at all points, as did the CVI in the patient group, we could not find a statistically significant difference.

The limitations of our study include the relatively small sample size and absence of detailed ocular examinations due to the logistic challenges of managing patients with COVID-19. Binarization of choroidal images was performed only in the right eye of each participant; therefore, inter-eye differences might have affected the results.

In conclusion, this study is the first to show that a significant transient decrease in choroidal vascular and structural parameters can occur during the acute phase of COVID-19. Further studies with a larger sample size are needed to clarify the choroidal structural and vascular changes and determine the ocular blood flow changes in patients with COVID-19.

REFERENCES

1. Lai CC, Shih TP, Ko WC, Tang HJ, Hsueh PR. Severe acute respiratory syndrome coronavirus 2 (SARS-CoV-2) and coronavirus disease-2019 (COVID-19): the epidemic and the challenges. *Int J Antimicrob Agents*. 2020;55(3):105924.
2. European Centre for Disease Prevention and Control. Geographical distribution of 2019-nCoV cases. [cited 2020 Jan 26]. Available from: URL: <https://www.ecdc.europa.eu/en/geographical-distribution-2019-ncov-cases>.
3. Tufan A, Avanoğlu Güler A, Matucci-Cerinic M. COVID-19, immune system response, hyperinflammation and repurposing antirheumatic drugs. *Turk J Med Sci*. 2020;50 SI-1:620-32.
4. Leisman DE, Deutschman CS, Legrand M. Facing COVID-19 in the ICU: vascular dysfunction, thrombosis, and dysregulated inflammation. *Intensive Care Med*. 2020;46(6):1105-8.
5. Wu P, Duan F, Luo C, Liu Q, Qu X, Liang L, et al. Characteristics of Ocular Findings of Patients With Coronavirus Disease 2019 (COVID-19) in Hubei Province, China. *JAMA Ophthalmol*. 2020;138(5):575-8.
6. Chen L, Liu M, Zhang Z, Qiao K, Huang T, Chen M, et al. Ocular manifestations of a hospitalised patient with confirmed 2019 novel coronavirus disease. *Br J Ophthalmol*. 2020;104(6):748-51.
7. Sommer A. Humans, viruses, and the eye-an early report from the COVID-19 front line. *JAMA Ophthalmol*. 2020;138(5):578-9.

8. Seah I, Agrawal R. Can the Coronavirus Disease 2019 (COVID-19) Affect the Eyes? A Review of Coronaviruses and Ocular Implications in Humans and Animals. *Ocul Immunol Inflamm.* 2020;28(3):391-5.
9. Casagrande M, Fitzek A, Püschel K, Aleshcheva G, Schultheiss HP, Berneking L, et al. Detection of SARS-CoV-2 in Human Retinal Biopsies of Deceased COVID-19 Patients. *Ocul Immunol Inflamm.* 2020;28(5):721-5.
10. Kurup SP, Khan S, Gill MK. Spectral domain optical coherence tomography in the evaluation and management of infectious retinitis. *Retina.* 2014;34(11):2233-41.
11. Marinho PM, Marcos AA, Romano AC, Nascimento H, Belfort R Jr. Retinal findings in patients with COVID-19. *Lancet.* 2020;395(10237):1610.
12. Sonoda S, Sakamoto T, Yamashita T, Shirasawa M, Uchino E, Terasaki H, et al. Choroidal structure in normal eyes and after photodynamic therapy determined by binarization of optical coherence tomographic images. *Invest Ophthalmol Vis Sci.* 2014;55(6):3893-9.
13. Loon SC, Teoh SC, Oon LL, Se-Thoe SY, Ling AE, Leo YS, et al. The severe acute respiratory syndrome coronavirus in tears. *Br J Ophthalmol.* 2004;88(7):861-3.
14. Yeo C, Kaushal S, Yeo D. Enteric involvement of coronaviruses: is faecal-oral transmission of SARS-CoV-2 possible? *Lancet Gastroenterol Hepatol.* 2020;5(4):335-7.
15. Seah IY, Anderson DE, Kang AE, Wang L, Rao P, Young BE, et al. Assessing viral shedding and infectivity of tears in coronavirus disease 2019 (COVID-19) patients. *Ophthalmology.* 2020;127(7):977-9.
16. Merad M, Martin JC. Pathological inflammation in patients with COVID-19: a key role for monocytes and macrophages. *Nat Rev Immunol.* 2020;20(6):355-62.
17. Kolb H. Simple Anatomy of the Retina. In: Kolb H, Fernandez E, Nelson R, editors. *Webvision: The Organization of the Retina and Visual System.* Salt Lake City (UT); 1995.
18. McLeod DS, Grebe R, Bhutto I, Merges C, Baba T, Lutty GA. Relationship between RPE and choriocapillaris in age-related macular degeneration. *Invest Ophthalmol Vis Sci.* 2009;50(10):4982-91.
19. Wei X, Sonoda S, Mishra C, Khandelwal N, Kim R, Sakamoto T, et al. Comparison of Choroidal Vascularity Markers on Optical Coherence Tomography Using Two-Image Binarization Techniques. *Invest Ophthalmol Vis Sci.* 2018;59(3):1206-11.
20. Agrawal R, Gupta P, Tan KA, Cheung CM, Wong TY, Cheng CY. Choroidal vascularity index as a measure of vascular status of the choroid: measurements in healthy eyes from a population-based study. *Sci Rep.* 2016;6(1):21090.
21. Oh J, Baik DJ, Ahn J. Inter-relationship between retinal and choroidal vasculatures using optical coherence tomography angiography in normal eyes. *Eur J Ophthalmol.* 2020;30(1):48-57.
22. Ruiz-Medrano J, Ruiz-Moreno JM, Goud A, Vupparaboina KK, Jana S, Chhablani J. Age-related changes in choroidal vascular density of healthy subjects based on image binarization of swept-source optical coherence tomography. *Retina.* 2018;38(3):508-15.
23. Singh SR, Vupparaboina KK, Goud A, Dansingani KK, Chhablani J. Choroidal imaging biomarkers. *Surv Ophthalmol.* 2019;64(3):312-33.
24. Wei X, Ting DS, Ng WY, Khandelwal N, Agrawal R, Cheung CM. Choroidal vascularity index: a novel optical coherence tomography based parameter in patients with exudative age-related macular degeneration. *Retina.* 2017;37(6):1120-5.
25. Agrawal R, Salman M, Tan KA, Karampelas M, Sim DA, Keane PA, et al. Choroidal vascularity index (CVI)-a novel optical coherence tomography parameter for monitoring patients with panuveitis? *PLoS One.* 2016;11(1):e0146344.
26. Agrawal R, Li LK, Nakhate V, Khandelwal N, Mahendradas P. Choroidal vascularity index in Vogt-Koyanagi-Harada disease: an EDI-OCT derived tool for monitoring disease progression. *Transl Vis Sci Technol.* 2016;5(4):7.
27. Agarwal A, Agrawal R, Khandelwal N, Invernizzi A, Aggarwal K, Sharma A, et al. Choroidal structural changes in tubercular multifocal serpiginoid choroiditis. *Ocul Immunol Inflamm.* 2018;26(6):838-44.
28. Liu S, Du L, Zhou Q, Zhang Q, Hu K, Qi J, et al. The choroidal vascularity index decreases and choroidal thickness increases in vogt-koyanagi-harada disease patients during a recurrent anterior uveitis attack. *Ocul Immunol Inflamm.* 2018;26(8):1237-43.